29. GEOTHERMAL MEASUREMENTS FROM DRILLING OF SEDIMENTS NEAR THE GALAPAGOS SPREADING CENTER, 86°W, DEEP SEA DRILLING PROJECT LEG 70[1]

Keir Becker, Deep Sea Drilling Project, Scripps Institution of Oceanography, La Jolla, California
R. P. Von Herzen, Woods Hole Oceanographic Institution, Woods Hole, Massachusetts
and
S. Karato, Ocean Research Institute, University of Tokyo, Nakano, Tokyo 164, Japan

ABSTRACT

Heat transfer processes at the mounds area of the Galapagos Spreading Center at 86°W are revealed by temperatures measured at $\approx$10-meter intervals in the 30 ± 10 meter sediment at each of 12 holes at Leg 70, Sites 506–509. Two hundred fourteen needle-probe values show a significant linear increase of thermal conductivity with depth in each hole. About half of the temperature–thermal resistance profiles are nonlinear and are fit to a steady-state, vertical pore-water convection model. Results indicate high and variable total heat flow and localized hydrothermal discharge at $\leq 10^{-8}$ m/s, associated with individual mounds. Recharge at similar rates is indicated in the low heat-flow belt $\approx$5 km south of the mounds. Possible slow entrained recharge within 100 meters of discharging mounds is suggested. At Site 510, temperatures in the 114-meter sediment cover on 2.7 million-year old crust are linear, suggesting that the hydraulic resistance of this layer is sufficient to seal off free hydrothermal exchange between basement and bottom water. The combination of heat-flow data and physical-properties data of Karato and Becker (this volume) suggests that $\approx$50 meters of sediment may be a threshold thickness for sealing of hydrothermal circulation within basement, where the topography is smooth. We suggest that the formation of mounds may be associated with the forced localization of hydrothermal discharge through the sediment, as its thickness approaches this threshold value.

INTRODUCTION

The hydrothermal mounds of the Galapagos Spreading Center (GSC) at 86°W longitude are set within the confines of one of the most detailed geothermal surveys on Earth. Several hundred oceanic heat flow measurements within $\approx$600 km^2 reveal the surface effects of an active crustal hydrothermal system (Sclater and Klitgord, 1973; Williams et al., 1974; Williams et al., 1979; Green et al., 1981). The two-dimensional variation of surface heat flow in this area provides a strong boundary condition for models of both mounds formation (e.g., Williams et al., 1979) and the spreading center hydrothermal system (Green, 1980). However, most of these surface heat flow values were obtained with 3- or 4-thermistor, 2- or 3-meter long probes, which give reliable measurements of surface conductive heat flux, but can only poorly resolve the processes of vertical heat transfer in the thin sediment layer.

During Leg 70, the deep-penetrating capabilities of the Deep Sea Drilling Project (DSDP) downhole temperature probe provided a unique opportunity to sample the vertical temperature field throughout the few tens of meters of sediment overlying the young crust of the GSC. The major objectives of these measurements were to obtain better resolution of the conductive and advective modes of heat transport and to apply the results to the problems of mounds development and the oscillatory pattern of surface heat flow. Despite relatively large experimental errors, our data show clear indications of local nonlinearities in the vertical temperature gradients. After correcting the data for well-resolved vertical variations in thermal conductivity, we interpret sediment temperatures in terms of a one-dimensional advection–conduction model.

GEOTHERMAL SETTING

For 20 years, heat flow measurements near spreading centers have been noted for considerable scatter about high mean values. This variance, and the failure of mean values to match plate tectonic predictions, are generally attributed to the unmeasured advection of heat through and from the young oceanic crust by hydrothermal circulation. Several years of detailed heat flow surveys on the south flank of the GSC at 86°W have revealed, with adequate sampling, a coherent, two-dimensional variation of heat flow resulting from hydrothermal processes (Sclater and Klitgord, 1973; Williams et al., 1974, Green et al., 1981). The latter two studies have shown that this pattern is oscillatory perpendicular to, and lineated parallel to, the spreading axis. Green (1980) has quite successfully modeled the heat flow variation normal to the axis, with hydrothermal circulation in a two-dimensional permeable layer, with material parameters and boundary conditions appropriate for a spreading plate model.

Green's (1980) results show that the GSC hydrothermal system is strongly dominated by axial processes; on the rise flanks, the cellular circulation tends to move with the spreading plate. As the crust migrates and ages, its thickening sediment cover becomes an increasingly

[1] Honnorez, J., Von Herzen, R. P., et al., *Init. Repts. DSDP*, 70: Washington (U.S. Govt. Printing Office).

important boundary layer between the basement circulation system and the effectively isothermal bottom water. As the sediment cover thickens relative to basement topography, free hydrothermal exchange between bottom water and basement is inhibited, which is reflected in the approach of measured conductive heat flow to predicted values (e.g., Lister, 1972; Sclater et al., 1974, Sclater et al., 1976; Anderson and Hobart, 1976). Anderson and Hobart (1976), considering regionally averaged data, show that the transition to a conductive regime occurs at a relatively young age for the GSC, 4-6 m.y., probably because of the relatively high sedimentation rate and smooth topography. At this age, the sediment cover here is about 200 meters. More locally, at 86°W, the measured heat flow is quite close to the theoretical value at about 1 m.y., where the sediment is about 50 meters thick (Williams et al., 1974; Williams et al., 1979). Physical properties of the sediments, particularly porosities (Karato and Becker, this volume), suggest that 50 meters is the approximate threshold thickness required for "sealing" of hydrothermal circulation within basement in areas away from topographic or tectonic conduits (faults) to the bottom water.

The mapped hydrothermal mounds at the GSC occur in 30 to 50 meters of sediment, within two bands characterized by high conductive heat flow about 20 and 30 km south of the spreading axis (Fig. 1) (Lonsdale, 1977; Williams et al., 1979; Green et al., 1981). A narrow heat flow low separates these two heat flow highs. These heat flow extrema are pronounced enough to seem to require hydrothermal discharge and recharge through the sediments. While *Alvin* submersible divers did not observe venting at the mounds, slow discharge of pore waters in the mounds region is indicated by six piston-core heat flow stations (Corliss et al., 1979) and by *Alvin* temperature probe data at individual mounds (Williams et al., 1979).

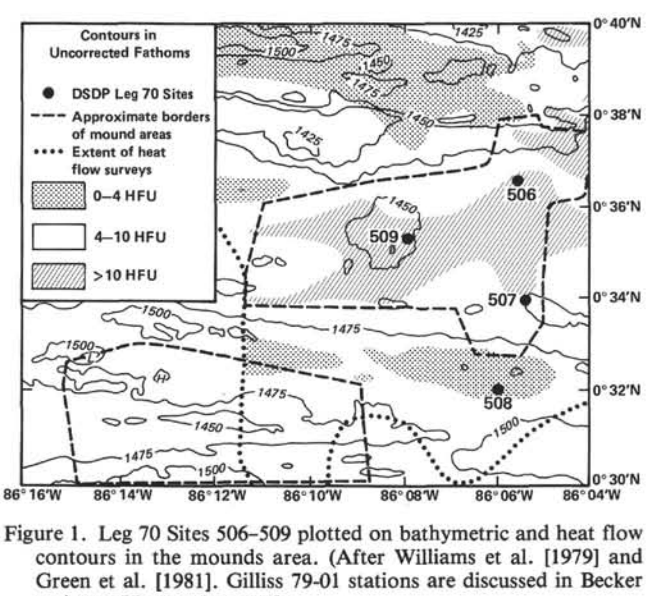

Figure 1. Leg 70 Sites 506–509 plotted on bathymetric and heat flow contours in the mounds area. (After Williams et al. [1979] and Green et al. [1981]. Gilliss 79-01 stations are discussed in Becker and Von Herzen [in press].)

HEAT FLOW MEASUREMENT LOCATIONS

Four of the five Leg 70 GSC sites were located in the mounds area, within a single cycle of the oscillatory heat flow pattern. They are plotted in Figure 1 on a heat flow contour map after Williams et al. (1979) and Green et al. (1981). Sites 506, 507, and 509 were located in separate concentrations of mounds within the same broad heat flow high. At each site, several holes were cored, both on and off mounds, by the hydraulic piston corer (HPC); thermal conductivities were measured in detail on these cores. In addition, undisturbed sediment was penetrated several times, offset slightly ($\lesssim$10–20 m) from the cores, solely for pore-water/sediment temperature measurements. These stations were called "holes" and assigned alphabetic suffixes (e.g., Hole 506E was the location of a heat flow measurement adjacent to the mound HPC Hole 506B). Site 508 was located in the heat flow low to the south, where three separate heat flow measurements were made in different holes. At these four locations particular attention was paid to interpretation of nonlinear temperature profiles in terms of hydrothermal processes in the sediment boundary layer. The fifth Leg 70 site, Site 510, was positioned about 95 km north of the spreading axis, in 114 meters of sediment, and thus provided a test of the sealing effect of this intermediate sediment thickness on the hydrothermal system.

TEMPERATURE MEASUREMENT

Sediment temperatures were measured using the DSDP downhole temperature probe developed for Leg 60 (Yokota et al., 1980) and subsequently modified with a longer and thinner sensor probe for greater penetration and faster time constant. This device records, at 128 one- or two-minute intervals, the resistance of a single thermistor to a precision of 10 ohms, providing nominal temperature resolution of 0.01 to 0.02°C. The thermistor is encased in a 1.25-cm diameter (= 2a) stainless steel tip, with a time constant ($a^2/\varkappa$) of about 2 to 3 minutes, depending on the sediment thermal diffusivity $\varkappa$. It protrudes about one meter below the drill bit and can be pushed into soft sediments beneath the bottom of the hole which are usually undisturbed by the drilling process or the presence of the massive drill pipe (Erickson et al., 1975).

Various station procedures were followed, depending on the drill string configuration and on the scientific objectives of the site. At Sites 506–509, where sediments were recovered by HPC and where basement drilling was attempted with a rotary drill bit, heat flow stations were separate "holes" located adjacent to HPC holes. In the 20 to 40 meters of sediment at these heat flow holes, two or three temperature determinations were made, at 8 to 10 meter intervals, by lowering the drill string into the soft mud the length of a single 8 to 10 meter section of pipe and holding for about 10 minutes. On the other hand, the 114 meters of sediment at Site 510 were drilled and partially cored; at three separate stages of drilling, the temperature probe was lowered down the pipe and pushed into undisturbed sediment ahead of the bit for single temperature readings.

Specific station procedures also varied with the bottom-hole assembly (BHA) used and had an important effect on measurement errors. Two kinds of BHA were used: a normal rotary drilling bit assembly and the assembly for hydraulic piston coring. The downhole probe was rigidly latched into the rotary drilling assembly, but it was only seated into the HPC assembly, with fluid pressure required to maintain probe position. Thus the probe position relative to the drill pipe is securely fixed with the rotary bit assembly, but it is not so secure with the BHA of the hydraulic piston corer. Moreover, the HPC assembly did not allow drill fluid washing ahead of the bit, to ease pushing the pipe into the sediments. However, the sediments at Site 506–509 were so porous and weak that the probe position probably did not vary significantly with respect to the BHA in any station.

The probe could either be dropped free down the pipe or lowered on a wire. The latter proved to be slower but safer: Twice the probe was damaged during free falls. However, the wireline prevented the addition of pipe to the drill string during measurements. Hence, wireline measurements often did not extend as deep and sometimes produced only two sediment temperature points. In any thicker sediments this might have been a more serious limitation. The various combinations of operational procedures used during our heat flow measurements are summarized in Table 1.

Temperature–time records for our stations are presented in Figure 2. Several sources of error limited the precision of our gradient determinations to 0.01 to 0.1 degrees per meter, depending on the uncertainties of individual temperature measurements, which varied from $\pm 0.1°$ to as much as $\pm 1.5°$. Equilibrium sediment temperatures were estimated by regressions against both the first and second order approximations (Blackwell, 1954) to Bullard's (1954) F-function, which describes the decay of the frictional heating of a cylindrical probe on penetration. Estimated errors in individual temperature determinations correspond to the standard errors of these regressions. These errors were on the order of five

Table 1. Methods used during heat flow stations.

Hole	Bottom-Hole Assembly	Wireline or Free Fall	Heave Compensator	Wash through Sediments
506E	HBR	Free fall	No	Yes
506F	HBR	Wireline	No	Yes
507A	HBR	Free fall	Yes	
507E	HPC	Free fall	No	Yes
507G	HPC	Free fall	No	Yes
507I	HPC	Wireline	No	
508A	HPC	Wireline	No	No
508D	HBR	Wireline		No
508E	HBR	Free fall		No
509A	HPC	Free fall	No	
509C	HPC	Wireline	No	No
509D	HPC	Wireline	No	
510	HBR	Wireline	Yes	Yes

Note: HBR = hydraulic bit release for rotary drilling; HPC = hydraulic piston core.

to ten times greater than the differences in temperatures obtained with the two approximations. In Figure 2 we present plots of the first order regressions (temperatures versus inverse time) which allow a subjective assessment of the data quality. All results reported here were obtained with the second order approximation, which is very close to the F-function for times greater than two or three probe time constants (Huppert and Sclater, 1966).

In several cases, thermistor temperatures showed very little apparent frictional heating on emplacement in the sediment, but instead behaved like measurements in water (e.g., Erickson et al., 1975). This probably resulted from the extremely porous and unconsolidated nature of the thin sediments (Karato and Becker, this volume), resulting in negligible frictional effects, so that these data are representative of real sediment temperatures.

Some temperature measurements show large variations at times when we attempted to hold the probe stationary in the sediment and after frictional effects should have diminished. These disturbances are reflected by sudden discontinuities in the temperature–time and temperature–inverse time plots of Figure 2. We attribute these problems to two disturbances: continued motion of the probe and circulation of cold drilling water about the probe. Because our measurements were made at shallow depths in wet, incompetent sediment that could not support the BHA, ship movements were transmitted to the probe. Use of the ship's drill-string heave compensator on a few stations produced some improvement in the temperature records. This problem may have been mitigated to some extent by relatively low frictional heating generated by movement through the weak sediments. Water circulation about the probe was troublesome during early stations when the pipe was lowered with partial washing; the first station (506E) was the worst case.

Smaller, generally consistent gradient errors arose from limitations to the precision of sub-bottom depth and temperature measurements. Drill string lengths are quite accurately recorded, but resolution of mudline depth in that coordinate system is limited in the heat flow "holes" where no coring was done. Most of these holes were placed within 20 to 30 meters of the HPC holes, and mudline depths from these coring sites were assumed to hold to ± 0.5 meter for heat flow measurements. During a few of the stations, a 12-kHz pinger was attached outside the pipe, about 100 meters above the bit. Bottom reflection travel times verified our assumption of mudline depths from adjacent core mudlines to within ± 1 meter. We estimate a general error range of 1 meter for our sub-bottom depth values, which resulted in a significant limitation on the precision of our heat flow calculations in the thin sediments.

Limitations in the instrumental resolution of temperature were probably much less significant than were errors resulting from operational disturbance during measurements. The drill string was generally closed to circulation with bottom water, so we could not routinely check the thermistor calibration against the well-known bottom water temperature. However, at one station,

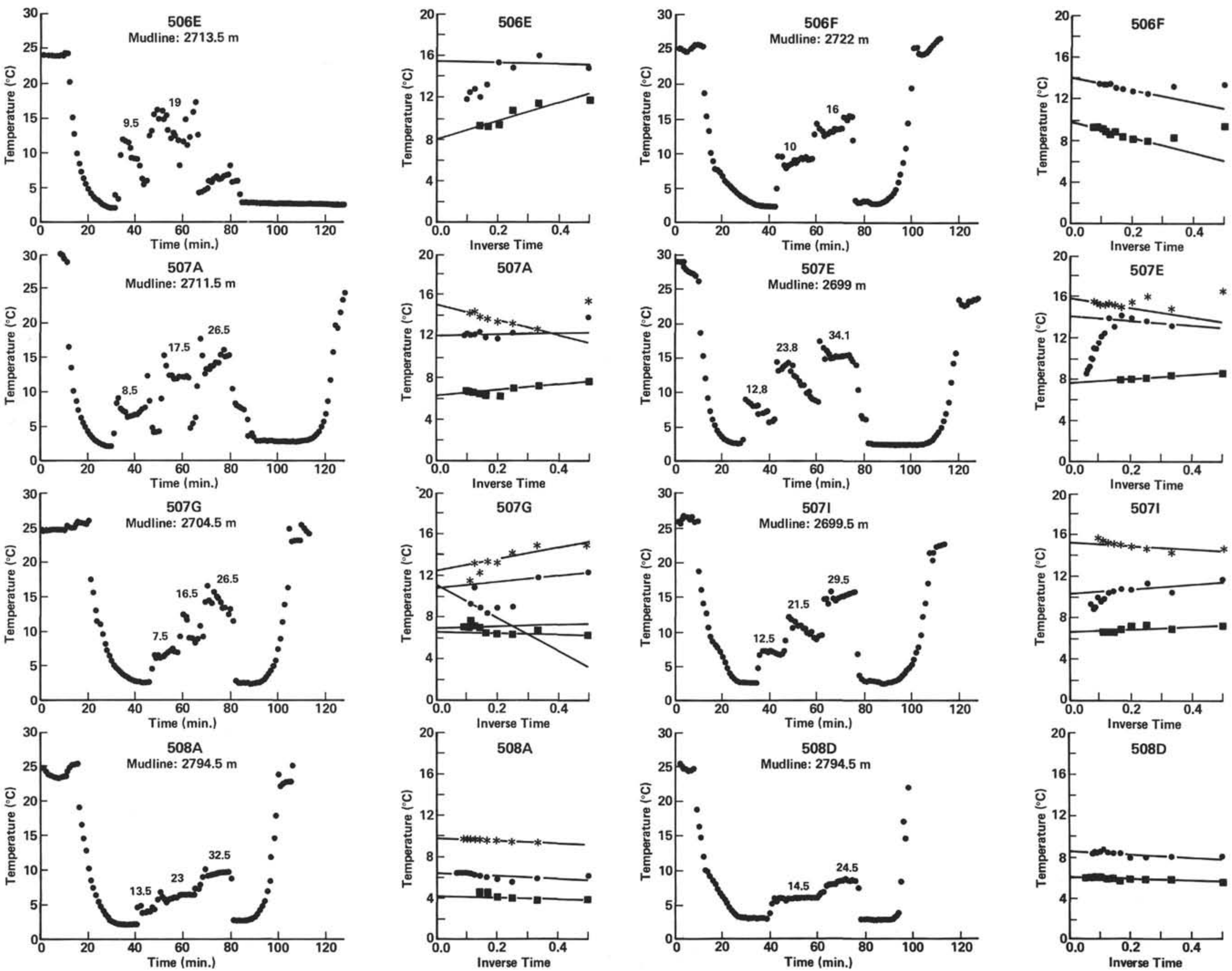
506E
Mudline: 2713.5 m
9.5
19
Temperature (°C)
Time (min.)
506E
Inverse Time
506F
Mudline: 2722 m
10
16
506F
507A
Mudline: 2711.5 m
8.5
17.5
26.5
507A
507E
Mudline: 2699 m
12.8
23.8
34.1
507E
507G
Mudline: 2704.5 m
7.5
16.5
26.5
507G
507I
Mudline: 2699.5 m
12.5
21.5
29.5
507I
508A
Mudline: 2794.5 m
13.5
23
32.5
508A
508D
Mudline: 2794.5 m
14.5
24.5
508D

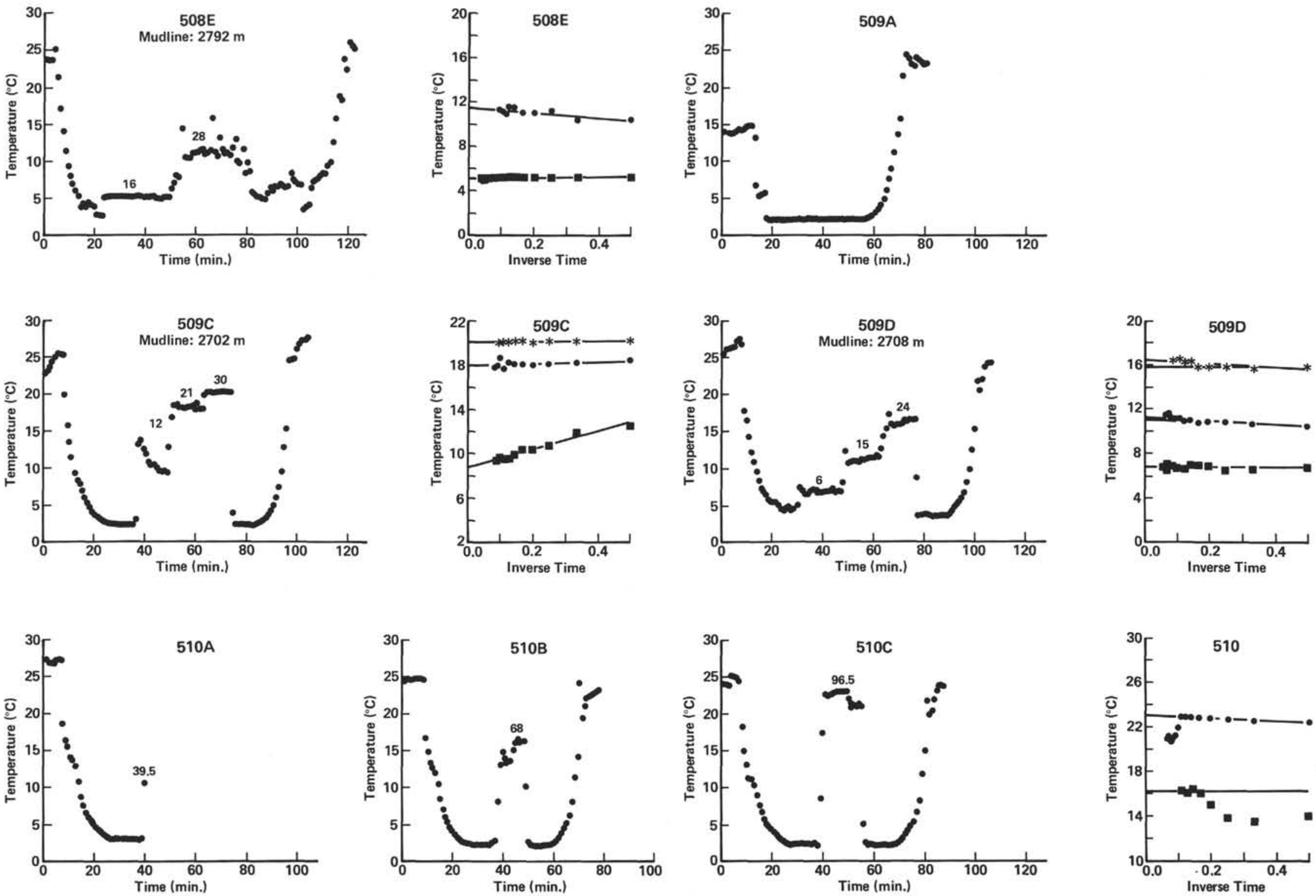

Figure 2. Heat flow station temperature-time records, and temperatures plotted against inverse time (min.$^{-1}$) for individual penetrations. (Mudline depth given in meters below rig floor, which is 9 m above water line. Also noted are sub-bottom depths in meters for separate temperature points.)

509A, the drill pipe was held above bottom while the probe was dropped. Somehow, as a result of this procedure, the probe never entered the sediment, since it registered within 0.05° of the bottom water temperature throughout the station. Based on this result, we estimate absolute instrumental temperature resolution to be about ±0.1°C throughout Leg 70, relatively insignificant in this region of high heat flow.

Jaeger's (1961) drill pipe heat-exchanger theory suggests that at the low pumping rates used on Leg 70, drilling fluid temperatures within the pipe at the mudline should be very close to bottom water temperatures. For all but two of our stations, mudline water temperatures in the pipe were within +0.5°C of bottom water temperature, which corroborates this theory and does not significantly contradict our estimated measurement accuracy. For the two anomalous stations, 508D and 509D, measured mud-line temperatures were about 1 and 2°C above bottom water, respectively. It was not clear how significant these mismatches were to the accuracy of subsequent temperature measurements in sediment, as no corrections were applied to the data. Indeed, the temperature data for these two stations seem to be of good quality (Figs. 2 and 4). Nevertheless, there exists the possibility of unknown instrumental or operational disturbances to these measurements, which may introduce additional errors in our interpretations of these two stations.

THERMAL CONDUCTIVITY MEASUREMENTS

Thermal conductivities of the sediments were measured at close intervals ($\lesssim$ 1–2 meters) in all cores by the needle-probe method of Von Herzen and Maxwell (1959). Disturbances to the hydraulic piston cores were minimal, so the laboratory conductivity values, corrected for pressure and temperature effects, are assumed to be representative of *in situ* values. Corrections for these effects to *in situ* conditions were made by the relations of Ratcliffe (1960) as modified by Hyndman et al. (1974).

Two instrument-related problems limited resolution of conductivities to no better than ±5%: (1) a slight deviation of the needle-probe temperature–time behavior from the theoretical form, suggesting improper internal heater wire or thermistor configuration, and (2) poor calibration of the needle-probe resistance with temperature. The first problem was evidenced by a consistent, slight curvature of the needle temperature response vs. log time, which should be linear for measurement times greater than 20 to 30 seconds (Jaeger, 1958; Von Herzen and Maxwell, 1959). The sense of this curvature was that temperature did not increase fast enough with log time, so that effects of finite sample size could be ruled out. All electronics used were carefully checked, and special care was taken to insure stable sample temperatures before measurement. Since calculated conductivity values are inversely proportional to the measured temperature rise, this effect produced larger conductivity values at later experimental times. It was minimized by calculating conductivities from a standardized early time interval (0.75–2.0 min.), with the expectation that absolute conductivity values might still be a few percent too high.

The other problem involved the fact that the needle-probe thermistors had not been properly calibrated. We calibrated their resistances on board the *Glomar Challenger* against the temperature of a well-calibrated heat flow probe; a subsequent recalibration one year later against a reliable quartz crystal oscillator corroborated the first to within 3 to 5%, but suggested that our conductivity values needed to be corrected upwards by about 4%. Since there is some question as to the accuracy of the temperature standard in the first calibration, and since the corrections for the two instrument-related problems roughly balance, we did *not* correct our shipboard values. These values are probably accurate to about 5 to 10%. The relative variations of conductivity downhole and between holes are much better determined, since a consistent experimental procedure was used.

Some confirmation of our estimated accuracy of conductivity values arises from a comparison of three large independent data sets of conductivity values of GSC 86°W sediments, measured with similar but independently constructed needle-probe apparatuses. Green et al. (1981) measured about 60 values on cores less than 10 meters long, and found a mean and standard deviation of 1.78 ± 0.07 mcal/cm•s•°C (0.75 ± 0.03 W/m•K). Becker and Von Herzen (in press) measured 113 values on piston cores to 10 meters length, with an average of 1.79 ± 0.07 (0.75 ± 0.03). The mean of our 68 values to 10-meters depth is 1.89 ± 0.12 (0.79 ± 0.05), which agrees within 5% with the other results, but again suggests that our values may be slightly high.

In situ thermal conductivities are plotted against depth for all cores in Figure 3. At every hole conductivities were found to increase with depth within about 30 meters of basement. In each case a linear increase of conductivity with depth fits the data better than a mean value, and the least-squares lines are also plotted on Figure 3. Statistics of the data fits are given in Table 2. Values of surface conductivity, K_0, display a rather large range, 1.59–1.90 mcal/cm•s•°C (0.66–0.79 W/m•K), suggesting that there may be significant lateral variations of conductivity at the GSC 86°W. Values of the slopes of the regressions cluster around 0.02 mcal/cm•s•°C/m (0.005 W/m•K/m), which is a very high depth gradient of conductivity. Karato and Becker (this volume) show that these gradients arise from high gradients in sediment porosity, which are significantly higher here than those observed in geothermally inactive sediments. These porosity gradients correlate with surface heat flows and are thus intimately related to hydrothermal processes. Karato and Becker (this volume) also discuss the interrelationship of conductivity values with other physical properties, and the variation of conductivity and other properties between hydrothermal and pelagic sediments.

Heat flows were calculated using the linear relationship of conductivity with depth. This was accomplished by transforming from depth to thermal resistance coordinates, using the change of variables first suggested by Bullard (1939):

$$R(z) = \int_0^z \frac{dz'}{K(z')} \tag{1}$$

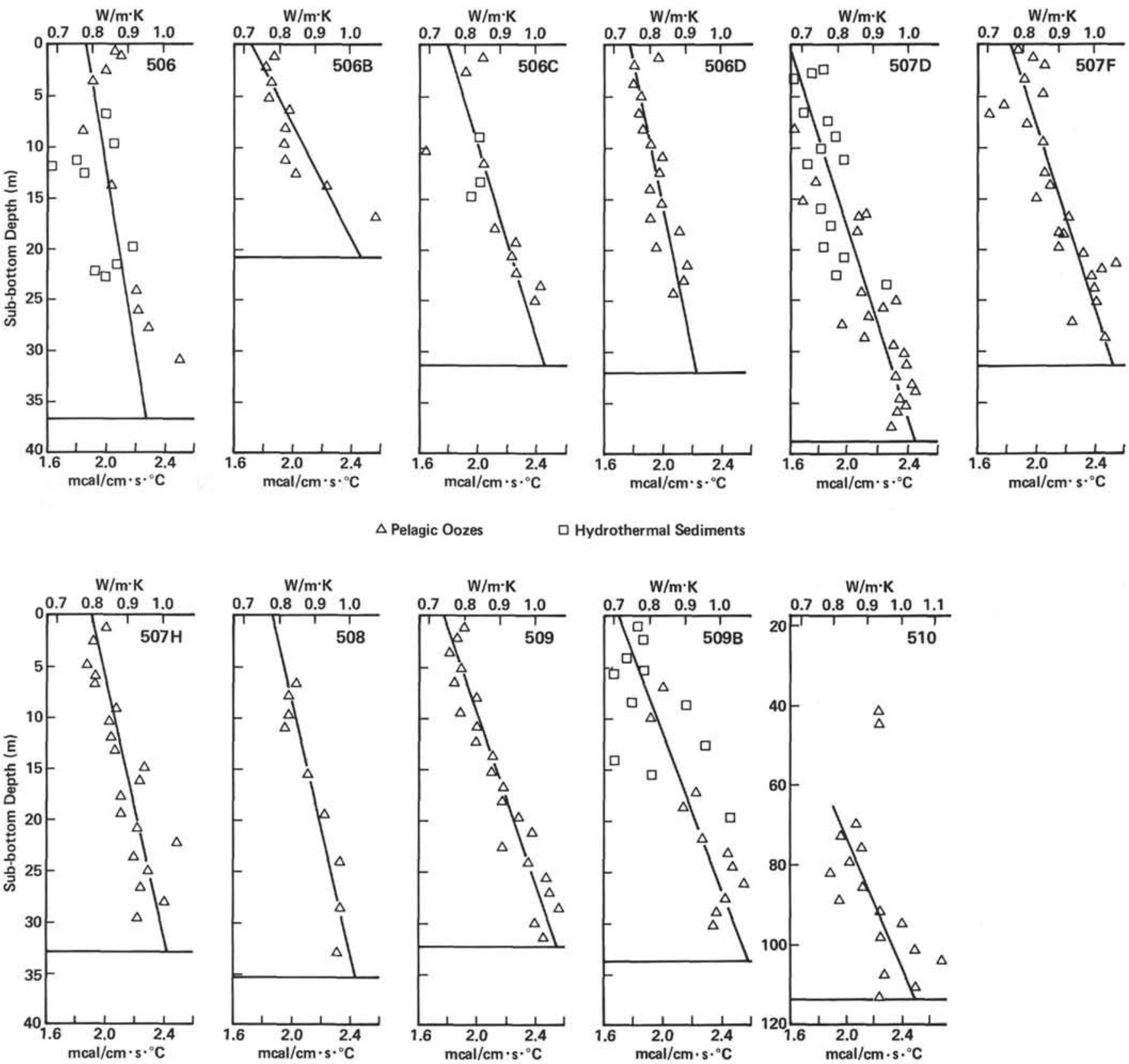

Figure 3. Thermal conductivity vs. sub-bottom depths for HPC's adjacent to heat flow stations. (Squares are hydrothermal sediments; circles are pelagic oozes. Also shown are linear regressions of conductivity with depth; regression statistics are summarized in Table 2.)

Table 2. Galapagos Spreading Center 86°W thermal conductivity, Leg 70.

Station	No. Values	Mean (CGS: mcal/cm·s·°C)	S.D. (CGS: mcal/cm·s·°C)	$K(z)$ (CGS: mcal/cm·s·°C)	$S_{K/z}$	Mean (SI: W/m·K)	S.D. (SI: W/m·K)	$K(z)$ (SI: W/m·K)	$S_{K/z}$
506	19	2.04	0.20	1.88 + 0.011z	0.16	0.85	0.08	0.79 + 0.005z	0.07
506B	11	2.01	0.22	1.72 + 0.036z	0.12	0.84	0.07	0.72 + 0.015z	0.05
506C	13	2.10	0.21	1.79 + 0.021z	0.15	0.88	0.09	0.75 + 0.009z	0.06
506D	18	1.93	0.14	1.77 + 0.014z	0.09	0.81	0.06	0.74 + 0.006z	0.04
507D	38	2.02	0.27	1.59 + 0.022z	0.12	0.85	0.11	0.67 + 0.009z	0.05
507F	24	2.14	0.23	1.83 + 0.022z	0.12	0.90	0.09	0.77 + 0.009z	0.05
507H	20	2.13	0.17	1.90 + 0.016z	0.09	0.89	0.07	0.80 + 0.007z	0.04
508	9	2.14	0.16	1.87 + 0.016z	0.06	0.89	0.06	0.78 + 0.007z	0.03
509	22	2.15	0.24	1.77 + 0.024z	0.08	0.90	0.10	0.74 + 0.010z	0.03
509B	23	2.10	0.29	1.71 + 0.026z	0.16	0.88	0.12	0.72 + 0.011z	0.07
510	17	2.22	0.21			0.93	0.09		
$z<100$ m	12	2.12	0.15			0.89	0.06		
$z>50$ m	15	2.21	0.23	1.91 + 0.012z*	0.16	0.93	0.09	0.80 + 0.005z*	0.07
$z^* = z - 65$									

Note: S.D. = standard deviation; $S_{K/z}$ = standard error of fit of conductivity with depth; z in meters.
[a] Units of depth gradient of conductivity are thermal conductivity units per meter (i.e., mcal/cm·s·°C/m or W/m·K/m).

With a linear expression for conductivity, $K(z) = K_0 + bz$, this can be integrated, yielding:

$$R(z) = \frac{1}{b} \ln\left[\frac{K_0 + bz}{K_0}\right], \text{ with } K_0,\ b, z > 0 \qquad (2)$$

RESULTS

Despite rather large measurement errors our temperature data, plotted against integrated thermal resistance in Figure 4, suggest significant nonconductive processes in the sediments at the GSC. For a constant conductive heat flow, the observed linear increase of conductivity should be coupled with a corresponding decrease in temperature gradient with depth. Most of our temperature profiles were nonlinear with depth, but not always in the sense required for purely conductive heat flow. Those requiring other processes appear as nonlinear plots of temperature against thermal resistance.

A number of thermal processes could result in nonlinear temperature profiles within the sediment layer. Among the possibilities are: (1) variations in the boundary temperatures, either in the bottom water or at the sediment/basement contact; (2) heat sources or sinks within the sediment (e.g., chemical reactions); or (3) convection of pore waters through the sediments. Several years of heat flow work have demonstrated that the bottom water temperature is now stable in this region, but the stability of either bottom water or basement temperatures for periods longer than the conductive time constant of the sediment layer ($\simeq$100–200 y.) cannot be directly shown. However, our data show local variations in both the degree and sign of curvature of temperature profiles, which we take to rule out any plausible regional boundary temperature changes. It is unlikely that exothermic and endothermic chemical reactions in the sediments can be of sufficient magnitude and local variability to produce the temperature variations that we observe (e.g., Watanabe et al., 1975). We then interpret our results in terms of the hydrothermal processes which are strongly indicated to be responsible for the oscillatory variation of surface heat flow and for the formation of the mounds (e.g., Williams et al., 1974; Williams et al., 1979; Green et al., 1981). After Wooding (1960) and Bredehoeft and Papadopulos (1965), we treat our data as temperature samples within a porous boundary layer within which one-dimensional heat transfer processes are dominant.

HEAT TRANSFER IN THE SEDIMENT BOUNDARY LAYER

The equations governing fluid flow and heat transport in a porous medium are quite complicated and can generally only be handled numerically. Wooding (1960) has shown that, where these equations can be reduced to one-dimensional, steady-state form, an exponential boundary layer holds at the permeable surface normal to the direction of variation. This layer is stable for the slow fluid flow rates through the sediments deduced from our temperature measurements and is of thickness $K/w(\varrho c)_f$ (Wooding, 1960), where: K = matrix thermal conductivity; w = fluid volume flux/unit area (dimensions of velocity); and $(\varrho c)_f$ = fluid volumetric specific heat.

The conditions necessary for this exponential boundary layer to occur are particularly appropriate to the 30 to 50 meters of sediment at Sites 506–509, for the following reasons:

1) Karato and Becker (this volume) show that the vertical hydraulic resistance of the sediment layer is of the same order as the hydraulic resistance of the much thicker basement. Over horizontal distances greater than the sediment thickness, the lateral hydraulic resistance of the sediment must then be greater than that of the basement. The regular variation of surface heat flow suggests that lateral pressure gradients exist within the crust over scales of kilometers; at these scales, lateral darcian flows must be confined to the basement because of the disparity between lateral sediment and basement hydraulic resistances. Moreover, because of the aspect ratio of the sediment layer, vertical pressure gradients will be much larger than lateral gradients in the mud. Thus vertical darcian flows will predominate through the sediment.

2) Both the conductive and convective time constants for the sediment layer are on the order of 100 years, insignificant compared to probable variation times for a cellular basement hydrothermal system, estimated from the crustal ages required for peak-to-peak variation of surface heat flow. Thus vertical steady state may be assumed to hold locally within the sediment. Further justification for steady-state flow through the sediments is found in the detailed numerical modelling by Green (1980), who found that, after about 0.2 m.y., the basement hydrothermal system was fixed relative to the moving plate.

In the one-dimensional, steady-state exponential sediment boundary layer, heat transport is governed by:

$$0 = \frac{d}{dz}\left(K\frac{dT}{dz} - w\varrho cT\right) \qquad (3)$$

with z and w positive downwards.

This equation has been solved for the case of constant material parameters with two sets of boundary conditions. Bredehoeft and Papadopulos (1965) use:

$$T = 0 \text{ at } z = 0 \quad \text{and } T = T_L \text{ at } z = L, \qquad (4)$$

whereas Sleep and Wolery (1978) and Williams et al. (1979) use:

$$T = 0 \text{ at } z = 0 \text{ and}$$

$$q \equiv -K\frac{dT}{dz} + w\varrho cT = -q_0, \text{ constant for all } z$$

$$(q_0 \text{ positive upwards}). \qquad (5)$$

Within the boundary layer, use of either (4) or (5) should give consistent results.

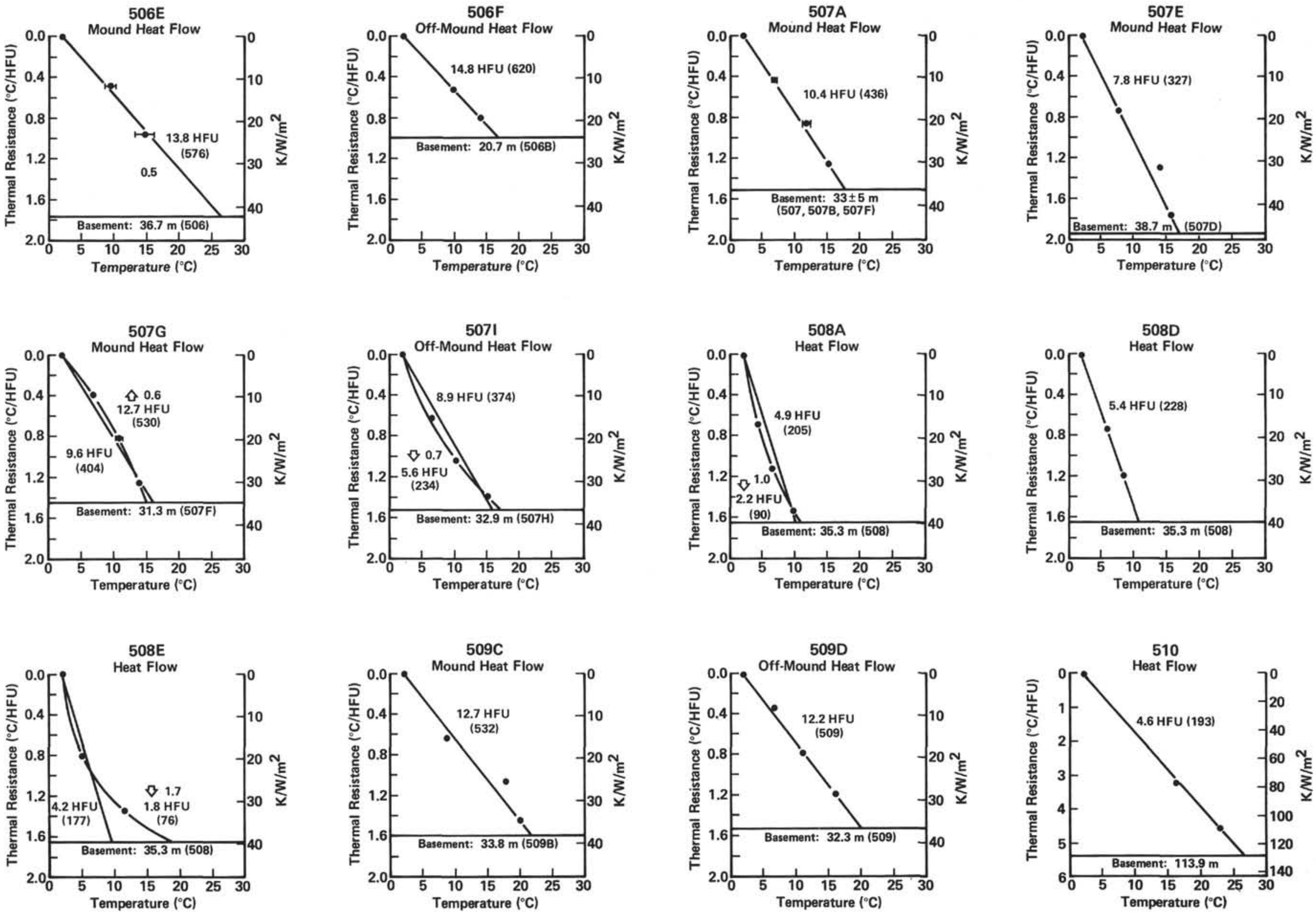

Figure 4. Temperatures vs. thermal resistance for Leg 70 heat flow stations. (Temperature error bars correspond to standard errors of regression lines against the cooling probe model. Straight lines are weighted least squares conductive fits to data; if present, curved lines are best fits to advective model (see Tables 3–5). Surface heat flows given for each model fit in heat flow units [= 10^{-6} cal/cm^2•s], with values in mW/m^2 in parentheses. Arrows indicate direction of advection at rate given in 10^{-8} m/s [10^{-8} m/s = 0.32 m/y.].)

For the general case where K, ϱc, and w may be arbitrary functions of depth, the general solution to (3) is

$$T = K_0 \left(\frac{dT}{dz}\right)_0 \int_0^z \frac{dy}{K} \exp\left(\int_0^y dx \frac{w\varrho c}{K}\right) \quad (6)$$

For the special case where $w\varrho c$ is constant, but conductivity varies with depth, (6) reduces to

$$T = \frac{K_0\left(\frac{dT}{dz}\right)_0}{w\varrho c} \exp\{w\varrho c R(z)\} - 1 \quad (7)$$

where $R(z)$ is defined by (1).

With the isothermal boundary conditions (4), (7) becomes

$$\frac{T}{T_L} = \frac{\exp\{w\varrho c R(z)\} - 1}{\exp\{w\varrho c R(L)\} - 1} \quad (8)$$

If the constant total flux condition (5) had been used:

$$T = \frac{q_0}{w\varrho c} \exp\{w\varrho c R(z)\} - 1$$
$$= \frac{q_0}{w\varrho c}\left\{\left(1 + \frac{bz}{K_0}\right)^{\frac{w\varrho c}{b}} - 1\right\} \quad (9)$$

Since the isothermal boundary condition at $z = 0$ requires all the heat transport to be conductive across the sediment-water interface, expression (9) is used to evaluate upwards surface conductive heat flow, as well as total heat flux across the sediment layer.

DATA INTERPRETATION

The temperature–depth data were fit in least-squares procedures to both the conductive and advective models. Unweighted and weighted formulations were used; both provide unbiased parameter estimates, but the latter yields the minimum variance estimates, where the model is known to describe reality. For our stations, we were uncertain about the appropriate models; comparison of relative magnitudes of misfits of data to the models was our main criterion for judging the appropriateness of the models to individual stations.

Since the data errors were dominated by variable errors in the individual temperature measurements, we assumed errors were uncorrelated, and derived weights from the estimated variances of the equilibrium sediment temperatures. Since some temperature measurements showed evidence for disturbances not accountable by the equilibrating probe model, we estimated the standard errors of the temperature measurements by the standard errors of fit of the regressions of equilibrating temperatures vs. the second order approximation (Blackwell, 1954) to Bullard's (1954) F-function. These estimates are shown as error bars in Figure 4 and are in good agreement with intuitive estimates of temperature errors from the station temperature–time records.

Moreover, these estimates are reasonable estimates of the standard errors of the intercept equilibrium temperatures, since the apparent periodicities of the noise processes in the temperature readings are longer than the temperature sampling interval. Hence the data are oversampled with regard to the noise processes, so fewer data points could contain the same information. Therefore the effective degrees of freedom in the data are considerably less than the numbers of data points. With both correlation coefficients and effective degrees of freedom near unity, the variances of the regression intercepts are very nearly the same as the variances of the fits of the regressions.

Within regression variances, the unweighted regression results agreed with the weighted results. Because of the range of errors in temperature measurements, we prefer the weighted results. Because of the errors in the temperature and conductivity measurements, surface heat flows are probably accurate to no better than ±10–20%. The sparsity of the data prevents statistically reliable estimates of error ranges in the reported heat flows. For the same reasons, we could not resolve fluid flux rates less than about 2×10^{-9} m/s, and errors in our estimates of these rates may be as high as $\pm 5 \times 10^{-9}$ m/s. With so few temperature–depth data points, misfit statistics for the two-parameter fits to the advective model were considered meaningless.

The results of the weighted and unweighted model-fitting are given in Tables 3–5. Data from each station were fit to the conductive model, with a linear increase

Table 3. Leg 70 heat flow results.

Station	Core	Corresponding Core Data Thermal Conductivity (z in meters)	Basement Depth (m)
506E	506 (mound)	1.88 + 0.011z(m)[a] 0.79 + 0.005z[b]	36.7
506F	506B (off-mound)	1.72 + 0.036z[a] 0.72 + 0.015z[b]	20.7
507A	507, 507B, 507F (mounds)	1.83 + 0.022z[a] 0.76 + 0.009z[b]	33 ± 5
507E	507D (mound)	1.59 + 0.022z[a] 0.66 + 0.009z[b]	38.7
507G	507F (mound?)	1.83 + 0.022z[a] 0.76 + 0.009z[b]	31.3
507I	507H (off-mound)	1.90 + 0.016z[a] 0.79 + 0.007z[b]	32.9
508A 508D 508E	508 (low heat flow, pelagic)	1.87 + 0.016z[a] 0.78 + 0.007z[b]	35.3
509C	509B (mound)	1.71 + 0.026z[a] 0.72 + 0.011z[b]	33.8
509D	509 (off-mound)	1.77 + 0.024z[a] 0.74 + 0.010z[b]	32.3
510	510 (pelagic)	2.12 ± 0.15[a] 0.89 ± 0.06[b]	113.9

[a] CGS units = mcal/cm•s•°C.
[b] SI units = W/m•K.

Table 4. Unweighted model fits.

	Conductive Model			Advective Model			
	Heat Flow		Basement Temperature	Total Heat Flow		Fluid Flow	Basement Temperature
Station	(HFU)	(mW/m^2)	(°C)	(HFU)	(mW/m^2)	(10^{-8} m/s)	(°C)
506E	13.38	560	25.7				
506F	14.74	617	16.8				
507A	10.52	440	16–20				
507E	8.24	345	18.1	9.2	385	D 0.2	17.6
507G	9.78	409	16.3	13.4	559	D 0.6	14.9
507I	8.69	364	15.4	5.3	224	R 0.8	17.4
508A	4.44	186	9.4	2.1	88	R 1.1	11.0
508D	5.45	228	11.1				
508E	6.19	259	12.3	1.7	73	R 1.8	19.0
509C	13.02	545	22.8	14.7	615	D 0.2	22.4
509D	12.00	503	20.3				
510	4.55	190	26.0				

Table 5. Weighted model fits.

	Conductive Model			Advective Model			
	Heat Flow		Basement Temperature	Total Heat Flow		Fluid Flow	Basement Temperature
Station	(HFU)	(mW/m^2)	(°C)	(HFU)	(mW/m^2)	(10^{-8} m/s)	(°C)
506E	13.61	570	26.4				
506F	14.80	620	16.9				
507A	10.41	436	16–20				
507E[a]	7.81	327	17.1				
507G	9.65	404	16.0	12.7	530	D 0.6	14.7
507I	8.93	374	15.8	5.6	234	R 0.7	17.4
508A	4.90	205	10.1	2.1	90	R 1.0	10.7
508D	5.44	228	11.1				
508E	4.23	177	9.8	1.8	76	R 1.7	18.2
509C[a]	12.71	532	22.0	18.4	772	D 0.6	21.2
509D	12.16	509	20.3				
510	4.60	193	26.8				

[a] Poor fit to either model.

of temperature with thermal resistance. In addition, six of the stations displayed consistently curved gradients, and the data from four of these stations could be successfully fit to the steady-state vertical advection model. (These six stations also had the worst standard errors of fit to the linear model.) In these cases, to estimate vertical fluid fluxes across the sediment layer, temperatures were fit to (9), using our experimentally determined values for K_0 and b, and a value of 1 cal/ $cm^3 \cdot °C$ (4.187 $MJ/m^3 \cdot K$) for the volumetric specific heat of the migrating fluid. Surface heat flows were obtained from these fits, and temperatures at the sediment/basement contact were derived by extrapolation with (9). Anderson et al. (1979) report experimental verification of this procedure for obtaining surface heat flow from curved temperature gradients. Note that for the flow rates obtained with this model the boundary layer thickness, defined as $K/w\varrho c$, is on the order of 50 meters, as is the sediment thickness. Thus these results are consistent with our treatment of the sediment as a stable boundary layer.

The two exceptional stations, Holes 507E and 509C, displayed similar strongly nonlinear temperature–depth samples. These data could not be satisfactorily fit to either the steady-state, one-dimensional conduction or advection models. The data are of reasonable quality for both stations, suggesting some inadequacy of these models in describing the thermal regimes at these holes. These are both mounds stations, where deep ($\approx$20 m sub-bottom) sections of hydrothermal sediments were cored. Both the temperature and the coring results could be consistent with some combination of lateral or transient discharge processes at these holes. Lateral channelling of vertically discharging thermal fluids could produce both the deep lenses of replacement hydrothermal sediments, as well as the observed nonexponentially convex-upwards temperatures.

Our preferred interpretation is that advective processes are active for the five stations, which are fit in a weighted sense to the steady-state, one-dimensional advection model, as well as for the exceptional stations, Holes 507E and 509C. Dominantly conductive heat flow is thought to occur at the other stations. On Figure 5, these preferred results are plotted on the mounds area map of Lonsdale (1977) for assessment of heat transfer processes associated with the mounds.

DISCUSSION

Our inaccurate temperature data cannot provide definite resolution among the many complicated geothermal processes that may occur in the sediments of the Galapagos Spreading Center. Nevertheless, most of the data can be fit adequately to simple one-dimensional heat transport models, which seem justified by both theory and results. Thus we interpret our results as evidence for surface manifestations of the ridge flank crustal hydrothermal system, previously inferred to be cellular from the pattern of surface heat flow (Williams et al., 1974; Williams et al., 1979; Green et al., 1981).

Several important observations can be made from our results at Sites 506–509 (Table 3), in the vicinity of the hydrothermal mounds (Fig. 5):

1) Surface heat flows are very high and locally quite variable in the mounds field, as has been noted by Williams et al. (1979). This can only be attributed to a local variability of hydrothermal discharge processes, presumably controlled by the small-scale basement faults which underlie the mounds field (Lonsdale, 1977).

2) Locally variable hydrothermal discharge through the sediments is suggested at three of the five mounds heat flow stations: Holes 507E, 507G, and 509B. Steady-state vertical discharge at about 0.6×10^{-8}m/s ($\approx$20 cm/y.) is suggested at 507G; transient or lateral discharge at possibly higher rates may occur at 507E and 509C. Although not fit to the advective model, the data at another mound heat flow station, 507A, vary about a linear profile in a sense consistent with vertical discharge. Thus, individual mounds appear to be associated with local concentrations of hydrothermal discharge through the sediments.

3) At a distinctly off-mound location, 507I (within $\approx$50 m from cored mound 507H), local recharge is suggested, at rates less than 10^{-8} m/s. This corroborates a similar result from *Alvin* short-probe temperature measurements (Williams et al., 1979), with the suggestion that local discharge at mounds entrains nearby pore water recharge. However, the data at the two other off-mound stations, 506F and 509D, appear to reflect dominantly conductive off-mound heat transfer.

4) Despite the local variation of directions and rates of pore-water movement in the mounds field, extrapolated temperatures at the sediment/basement contacts at Sites 506, 507, and 509 agree within $\approx$10°C and also confirm the estimates of Williams et al. (1979). This would seem to indicate an upper limit for the basement

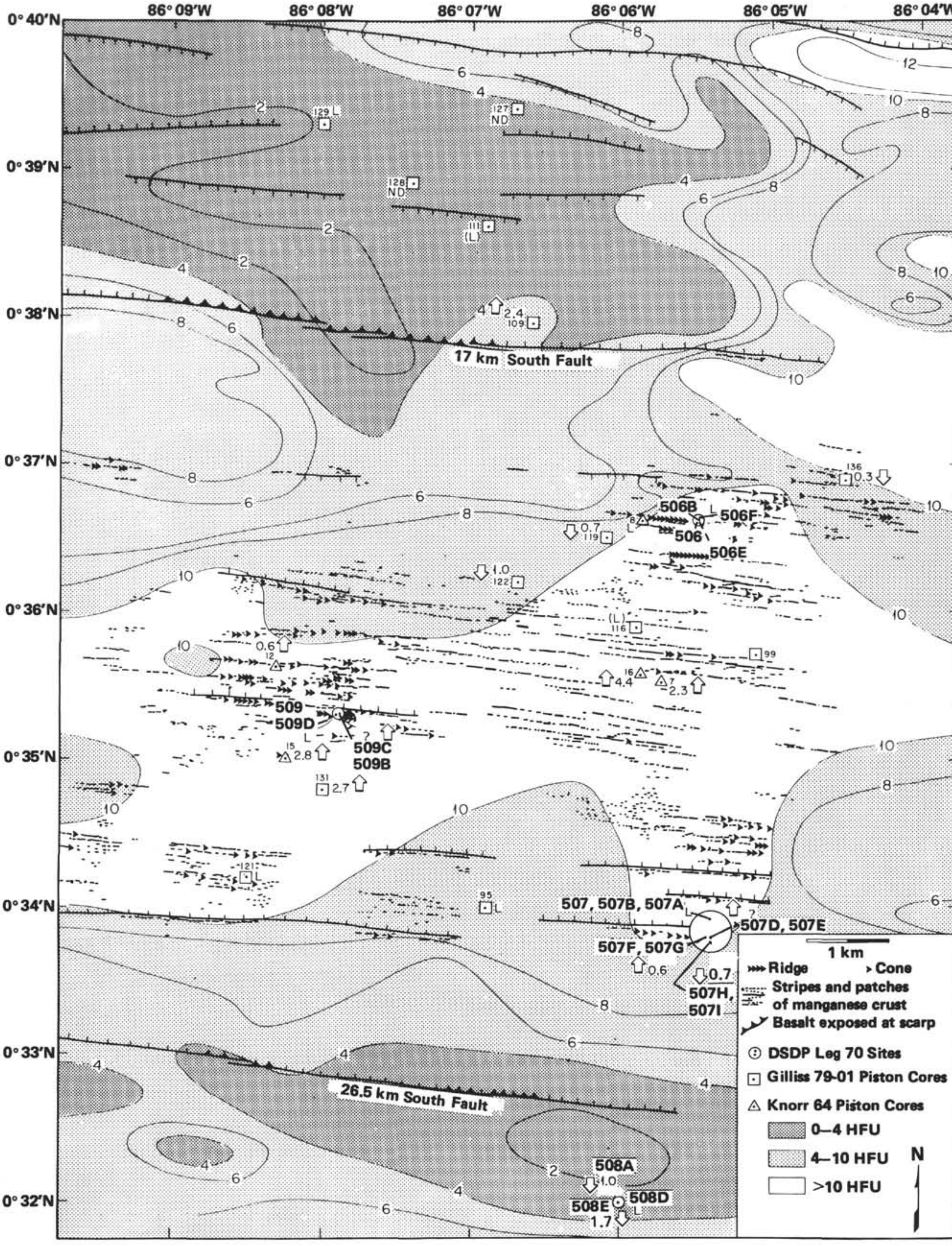

Figure 5. Stations and preferred model fits at Sites 506–509, located with respect to mapped mounds and faults, and heat flow contours, after Lonsdale (1977), Klitgord and Mudie (1974), Green et al. (1981), and Allmendinger and Riis (1980). (Also shown are advective model fits to piston core temperature data from Knorr 64 [Corliss et al., 1979; Williams et al., 1979; Green, 1980], and Gilliss 79-01 [Becker and Von Herzen, in press]. L indicates linear [conductive] temperature profile; (L) indicates only two data points; ND = no data. Discharge and recharge indicated respectively by upward- and downward-pointing arrows. Rates of discharge or recharge given in 10^{-8} m/s [10^{-8} m/s = 0.32 m/y.].)

exit temperatures of discharging thermal waters associated with the mounds, but the value of this limit probably depends critically on the precision of navigation with respect to the localized concentrations of discharge, as suggested by the two-dimensional models of Sleep and Wolery (1978) and Williams et al. (1979). If our stations were well-navigated in this regard, basement exit temperatures would probably be limited to 20 to 30°C; higher temperatures would be allowed if the navigation were of poorer quality.

5) At the low heat flow site, 508, recharge is indicated at rates similar to the mounds discharge rates. The inconsistencies among the results at Holes 508A, 508D, and 508E, all supposedly within a few tens of meters of 508, are puzzling. They probably reflect some combination of measurement and navigation errors and possibly local variability of recharge processes. (Hole 508D, with no apparent indications of recharge, is one of two stations with a bad mismatch of recorded mudline temperature and known bottom water temperature. If a shift in the thermistor/recorder temperature response were responsible, any correction would produce a recharge-type profile.) Local variability is more generally accepted for discharge patterns, but may also hold for recharge through the sediments if it is localized by discrete zones of high basement permeability. Moreover, the heat flow low within which Site 508 is located is apparently quite sharp (Figs. 1 and 5), which requires rapid lateral variations in the hydrothermal processes.

Site 510, while located in thicker sediment primarily for increased chances of basalt recovery, provided a good test site for the sealing effects of about 100 meters of sediment. However, the two deep temperature measurements here are inconclusive in this regard: within error limits, both a conductive regime and very slow recharge ($\lesssim 5 \times 10^{-10}$ m/s) are allowable. (Note that, because this site was only spot-cored, conductivity data are sparse over the depth range of the temperature measurements, and a constant value was used for the calculations. Any increase of conductivity with depth would exaggerate the concave-upward appearance of the temperature–thermal resistance profile in Fig. 4.) This area has not been well surveyed; available seismic profiles show smooth basement with even sediment cover. The measured heat flow, 4.5 HFU (190 mW/m^2), is only about two-thirds the value of 6.9 HFU (290 mW/m^2) (Parsons and Sclater, 1977) predicted for crust of the 2.67 m.y. estimated age at Site 510. However, the heat flow agrees quite well with values of 190–215 mW/m^2 about 15 to 30 km east, in a similar setting of smooth basement of similar age, draped by even sediment cover of 100 m (Sclater and Klitgord, 1973; Sclater et al., 1974). The consistency of these values suggests that heat transfer through ≈ 100 meters of sediment here must be dominantly conductive and that this thickness of sediment must be effectively impermeable to hydrothermal flow. However, the possibility of continued circulation within basement is suggested by the mismatch to the theoretical heat flow. We cannot rule out hydrothermal exchange with bottom water through possible unmapped basement highs and exposures, which might bypass the relatively impermeable sediment layer and result in low measured heat flow.

The pore-water convection rates we obtain in the mounds area are about an order of magnitude less than some reported by Anderson et al. (1979) on far older crust in the Indian Ocean, and one or two orders less than those derived by Williams et al. (1979) with a short probe from the submersible *Alvin* at the surfaces of individual mounds. We attribute this to a combination of factors which may also have a direct bearing on the formation of the mounds, in a manner similar to that proposed by Williams et al. (1979), as follows:

The topography of the Galapagos Rift at 86° is uncommonly smooth for a ridge flank, so that topographic control of hydrothermal circulation may be less important here, and the cellular nature of convection in a porous medium may be more developed. The basic pattern of a 1–2 km deep cellular system may be little affected by 100–200 meters of surface relief and up to 50 meters of sediment cover (see Green, 1980). However, the rapidly deposited sediment will strongly affect the surface expression of the hydrothermal system, particularly with respect to basement topography and structure. A thin sediment cover will have a greater sealing effect against a diffuse rather than a localized exchange of thermal fluids through the sediments; if thick enough, the sediment layer will force this exchange to be localized above basement highs and faults.

The physical properties of the sediments display both strong depth gradients, which increase the hydraulic impedance of the sediment layer, and a discontinuity in these gradients at about 30–50 meters above basement (Karato and Becker, this volume). We interpret these results as indicating that 30–50 meters of sediment have an important effect on the nature of the Galapagos hydrothermal system: the sediment strongly inhibits diffuse hydrothermal flow through the sediment and forces fluid transport through the sediment layer to be localized above discrete zones of maximum basement permeability. Convection through a sediment layer of thickness close to this apparent threshold sealing thickness may be subject to varying degrees of localization, depending partly on underlying basement structure. Thus our measured flow rates may be indicative of somewhat inhibited diffuse sediment pore water advection rates. On the other hand, the high mounds discharge rates of Williams et al. (1979) may reflect the very locally concentrated advection of thermal waters at the surfaces of the mounds, directly above small basement faults (Lonsdale, 1977).

We suggest that a critical factor for mounds formation may be the forced localization of hydrothermal discharge by the sediment cover. The physical properties data suggest that this occurs at about the sediment thickness of the mounds field, which would further suggest that the mounds may have formed recently and fairly rapidly. The particular combination of high sedimentation rate and smooth topography may allow mounds to form over a widespread area at the Galapagos Spreading Center, but similar hydrothermal features may be relatively rare at rougher, lesser-sedimented spreading centers.

ACKNOWLEDGMENTS

We thank the DSDP and GMI crew members who contributed to the success of the temperature conductivity measurements. Roy Hyndman, Marc Langseth, and Peter Lonsdale provided very helpful, constructive reviews of the manuscript. LeRoy Dorman greatly assisted in the statistical interpretation of the temperature data. We thank Lola Boyce for cheerfully typing several versions of the manuscript, and Jo Griffith for skillfully drafting the figures.

REFERENCES

Allmendinger, R. W., and Riis, F., 1979. The Galapagos Rift at 86°W: 1. Regional morphological and structural analysis. *J. Geophys. Res.*, 84:5379–5389.

Anderson, R. N., and Hobart, M. A., 1976. The relation between heat flow, sediment thickness, and age in the eastern Pacific. *J. Geophys. Res.*, 81(17):2968–2989.

Anderson, R. N., Hobart, M. A., and Langseth, M. G., 1979. Geothermal convection through oceanic crust and sediments in the Indian Ocean. *Science*, 204:828–832.

Becker, K., and Von Herzen, R. P., in press. Heat transfer through the sediments of the mounds hydrothermal area, Galapagos Spreading Center at 86°W. *J. Geophys. Res.*

Blackwell, J. H., 1954. A transient flow method for determination of thermal constants of insulating materials in bulk. *J. Applied Phys.*, 25:137–144.

Bredehoeft, J. D., and Papodopulos, I. S., 1965. Rates of vertical groundwater movement estimated from the Earth's thermal profile. *Water Resources Research*, 1(2):325–328.

Bullard, E. C., 1939. Heat flow in South Africa. *Proc. R. Soc. London Ser. A.*, 173:474–502.

________, 1954. The flow of heat through the floor of the Atlantic Ocean. *Proc. R. Soc. Lond.*, Ser. A, 222:408–429.

Corliss, J. B., Dymond, J., Gordon, L. I., Edmond, J. M., Von Herzen, R. P., Ballard, R. D., Green, K., Williams, D., Bainbridge, A., Crane, K., and Van Andel, Tj. H., 1979. Submarine thermal springs on the Galapagos Rift. *Science*, 203(4385):1073–1083.

Erickson, A. J., Von Herzen, R. P., Sclater, J. G., Girdler, R. W., Marshall, B. V., and Hyndman, R. D., 1975. Geothermal measurements in deep-sea drill holes. *J. Geophys. Res.*, 80:2515–2528.

Green, K. E., 1980. Geothermal processes at the Galapagos Spreading Center [Ph.D. dissert.]. Woods Hole Oceanographic Institution, Mass.

Green, K. E., Von Herzen, R. P., and Williams, D. L., 1981. The Galapagos Spreading Center at 86°W: A detailed geothermal field study. *J. Geophys. Res.*, 86(B2):979–986.

Huppert, H. E., and Sclater, J. G., 1968. On the *in situ* measurement of the thermal conductivity of deep-sea sediments. *Technical Memorandum* 191: La Jolla (Scripps Institution of Oceanography).

Hyndman, R. D., Erickson, A. J., and Von Herzen, R. P., 1974. Geothermal measurements on DSDP Leg 26. *In* Davies, T. A., Luyendyk, B. P., et al., *Init. Repts. DSDP*, 26: Washington (U.S. Govt. Printing Office), 451–463.

Jaeger, J. C., 1958. The measurement of thermal conductivity and diffusivity with cylindrical probes. *Trans. Am. Geophys. Union*, 39 (4):708–710.

________, 1961. The effect of the drilling fluid on temperatures measured in bore holes. *J. Geophys. Res.*, 66(2):563–569.

Klitgord, K. D., and Mudie, J. D., 1974. The Galapagos Spreading Center: A near-bottom geophysical study. *Geophys. J. Roy. Astron. Soc.*, 38:563–586.

Lister, C. R. B., 1972. On the thermal balance of a mid-ocean ridge. *Geophys. J. R. Astron. Soc.*, 26:515–535.

Lonsdale, P., 1977. Deep-tow observations at the mounds abyssal hydrothermal field, Galapagos Rift. *Earth Planet. Sci. Lett.*, 36: 92–110.

Parsons, B., and Sclater, J. G., 1977. An analysis of the variation of ocean floor bathymetry and heat flow with age. *J. Geophys. Res.*, 82(5):803–827.

Ratcliffe, E. H., 1960. The thermal conductivities of ocean sediment. *J. Geophys. Res.*, 65(5):1535–1541.

Sclater, J. G., Crowe, J., and Anderson, R. N., 1976. On the reliability of oceanic heat flow averages. *J. Geophys. Res.*, 81(17): 2997–3006.

Sclater, J. G., and Klitgord, K. D., 1973. A detailed heat flow, topographic, and magnetic survey across the Galapagos Spreading Center at 86°W. *J. Geophys. Res.*, 78(29):6951–6975.

Sclater, J. G., Von Herzen, R. P., Williams, D. L., Anderson, R. N., and Klitgord, K., 1974. The Galapagos Spreading Center: Heat flow low on the north flank. *Geophys. J. R. Astron. Soc.*, 38: 609–626.

Sleep, N. H., and Wolery, T. J., 1978. Egress of hot water from mid-ocean ridge hydrothermal systems: Some thermal constraints. *J. Geophys. Res.*, 83(B12):5913–5922.

Von Herzen, R., and Maxwell, A. E., 1959. The measurement of thermal conductivity of deep-sea sediments by a needle-probe method. *J. Geophys. Res.*, 64(10):1557–1563.

Watanabe, T., Von Herzen, R. P., and Erickson, A., 1975. Geothermal studies, Leg 31, Deep Sea Drilling Project. *In* Karig, D. E., Ingle, J. C., Jr., et al., *Init. Repts. DSDP*, 31: Washington (U.S. Govt. Printing Office), 573–576.

Williams, D. L., Green, K., Van Andel, Tj. H., Von Herzen, R. P., Dymond, J. R., Crane, K., 1979. The hydrothermal mounds of the Galapagos Rift: Observations with DSRV *Alvin* and detailed heat flow studies. *J. Geophys. Res.*, 84(B13):7467–7484.

Williams, D. L., Von Herzen, R. P., Sclater, J. G., and Anderson, R. N., 1974. The Galapagos Spreading Center: Lithospheric cooling and hydrothermal circulation. *Geophys. J. R. Astron. Soc.*, 38: 587–608.

Wooding, R. A., 1960. Rayleigh instability of a thermal boundary layer in flow through a porous medium. *J. Fluid Mech.*, 9: 183–192.

Yokota, T., Kinoshita, H., and Uyeda, S., 1980. New DSDP (Deep Sea Drilling Project) downhole temperature probe utilizing IC RAM (memory) elements. *Bull. Earthquake Res. Inst. Univ. Tokyo*, 54:441–462.